SUPPORTING INFORMATION

Photoresponsive Transformation from Spherical to Nanotubular Assembly: Anticancer Drug Delivery by Macrocyclic Cationic Gemini Amphiphiles

Subhasis Dey, Soumya Chatterjee, Anjali Patel, Nirmalya Pradhan, Diship Srivastava, Niladri Patra, Arindam Bhattacharyya, Debasis Manna*

Email: dmanna@iitg.ac.in

Table of Contents

Experimental Procedures

I. General information:

The reagents were procured from Sigma-Aldrich, Merck, and other commercial sources and used directly without further purification. Reactions were monitored by thin-layer chromatography (TLC) on silica gel 60 F254 (0.25 mm). The column chromatography was performed using 60–120 mesh silica gels. The ^{1}H NMR and ^{13}C NMR were recorded at 400 or 600 and 100 or 151 MHz with Varian AS400 spectrometer and Brucker spectrometer, respectively. The chemical shifts were reported in parts per million (δ) using DMSO-d_6, $CDCl_3$ as the internal solvent. The coupling constants (J values) and chemical shifts (δ_{ppm}) were reported in Hertz (Hz) and parts per million (ppm), respectively downfield from tetramethylsilane using residual chloroform (d = 7.28 ppm for ^{1}H NMR, d = 77.23 ppm for ^{13}C NMR) as an internal standard. Multiplicities are reported as follows: s (singlet), d (doublet), t (triplet), m (multiplet), and br (broadened). High-resolution mass spectra (HRMS) were recorded at Agilent Q-TOF mass spectrometer with Z-spray source using built-in software for analysis of the recorded data. Ultrapure water (Milli-Q system, Millipore, Billerica, MA) was used for the preparation of buffers. The stock solutions of compounds were prepared in gas chromatographic grade DMSO which was also purchased from Sigma.

II. Synthesis and characterization of the compounds

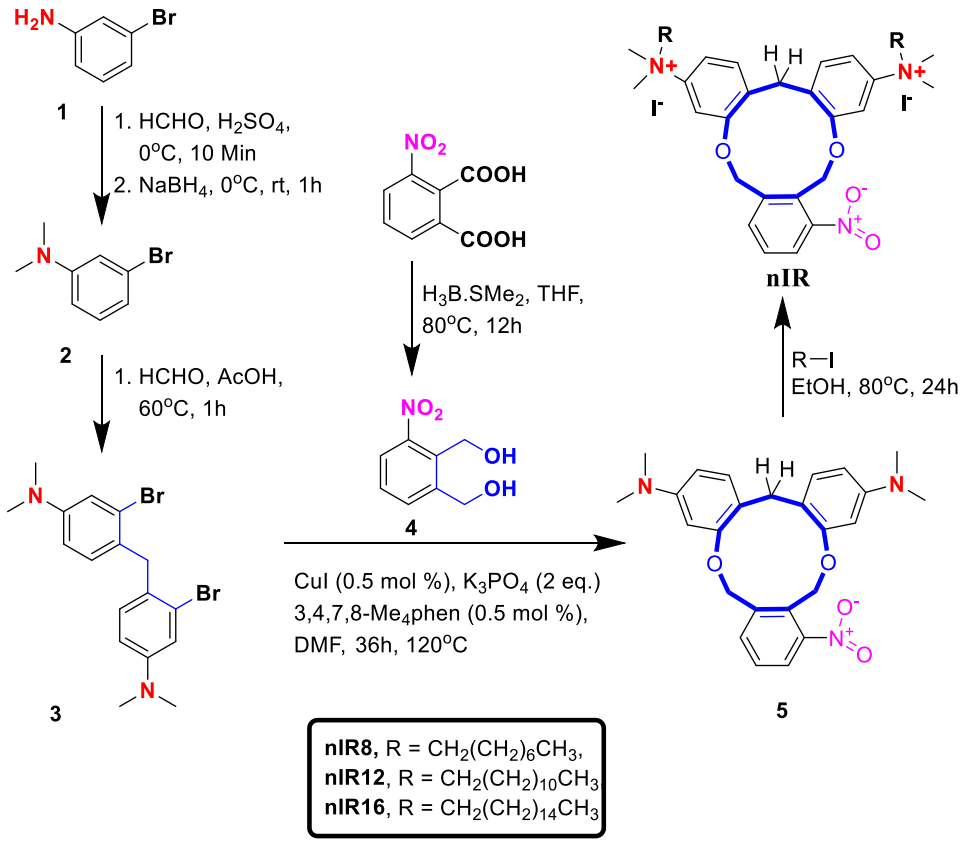

Scheme S1. Synthetic routes of the macrocyclic gemini cationic amphiphiles.

Synthesis of 3-bromo-N,N-dimethylanilin (2) – To a stirring solution of aqueous H_2SO_4 (3 M, 3.5 ml) and aqueous formaldehyde (37%, 1.30 mL, 17.43 mmol) in tetrahydrofuran (15 mL) at 0 °C was added 3-bromoaniline (1.0 g, 5.8 mmol), and the reaction mixture was stirred for 10 min. Then, solid $NaBH_4$ (0.88 mg, 23.25 mmol) was slowly added, and the temperature was maintained at 0 °C. After that, the resulting reaction mixture was allowed to warm up and stirred for 1 h at 20 °C. After maximum consumption of the starting materials, the reaction mixture was diluted with a saturated aqueous solution of $NaHCO_3$ (20 mL), and the reaction mixture was extracted with CH_2Cl_2 (3 × 20 mL). The combined organic layers were dried over anhydrous Na_2SO_4 and filtered, and solvents were evaporated under reduced pressure. The yellow crude product was of sufficient purity for the next step (yield: 1.173; 88%). The ^1H and ^{13}C NMR of the compound is in accordance with the literature report.[1]

Synthesis of 4,4'-methylenebis(3-bromo-N,N-dimethylaniline) (3) – To a stirring solution of 3-bromo-*N*,*N*-dimethylaniline (2, 1.0 g, 4.97 mmol) in glacial acetic acid (10 mL) aqueous formaldehyde (37%, 0.19 mL, 2.48 mmol) was added dropwise over 15 min. The reaction mixture was then stirred at 90 °C for 1-hour, and acetic acid was evaporated under reduced pressure. The residual acid was then neutralized with a saturated aqueous solution of $NaHCO_3$. After that, the reaction mixture was extracted with CH_2Cl_2 (3 × 20 mL). The combined organic layers were washed with water (2 × 20 mL) and brine (30 mL), dried over anhydrous Na_2SO_4, and filtered. The solvents were removed under reduced pressure. The resulting red liquid was purified through silica gel column chromatography using a gradient solvent system of ethyl acetate in hexane (0 – 10%) to provide the pure product as a white crystalline solid (yield: 0.74 mg; 88%). The ^1H and ^{13}C NMR of the compound is in accordance with the literature report.[1]

Synthesis of (3-nitro-1,2-phenylene)dimethanol (4) – To a stirring solution of 3-nitrophthalic acid (500 mg, 2.36 mmol) in dried THF was added 10 M solution of borane dimethylsulfide complex (dropwise addition; 2.5 equiv.). Then, the resulting solution was heated at 80 °C for 12 hours. After that, a 3 M aqueous solution of hydrochloric acid was added into this reaction mixture (dropwise) until effervescence was no longer observed. The resulting mixture was then extracted with 3 × 20 mL of ethyl acetate. The combined organic layers were washed with saturated aq. $NaHCO_3$ followed by brine. The resulting organic phase was dried over anhydrous Na_2SO_4 and filtered. The filtrate was concentrated under reduced pressure to afford the crude mixture. The mixture was purified through silica gel column chromatography with a solvent gradient system of 5–15% ethyl acetate in hexane to afford the pure compound 4. Characterization of the compound: Colorless solid (yield: 88%) ^1H NMR (600 MHz, $CDCl_3$) δ_{ppm} 8.20 – 8.14 (m, 1H), 7.59 – 7.50 (m, 2H), 5.55 (s, 2H), 5.22 (s, 2H); ^{13}C NMR (151 MHz, $CDCl_3$) δ_{ppm} 143.0,

136.3, 129.0, 127.0, 122.7, 74.0, 73.2; HRMS (ESI) calcd. for $C_8H_9NO_4$ $[M + K]^+$: 222.0169, found 222.0209.

Synthesis of N^3,N^3,N^{14},N^{14}-tetramethyl-7-nitro-6,11-dihydro-17H-tribenzo[c,g,j][1,6]dioxacycloundecine-3,14-diamine (5) – Compound 3 (500 mg, 1.21 mmol), (3-nitro-1,2-phenylene)dimethanol (489 mg, 2.66 mmol), K_3PO_4 (1.1g, 5.32 mmol), CuI (115 mg, 0.65 mmol,) and 3,4,7,8-tetramethyl-1,10-phenanthroline (142 mg, 0.65 mmol) were added to a screw capped seal tube under argon atmosphere. The tube was then evacuated and backfilled with nitrogen for three times. Then dry DMF (4 mL) was added by syringe at room temperature. The reaction mixture was stirred at 120^{o}C for 24 h. The reaction mixture was allowed to reach room temperature and then diluted with ethylacetate (20 mL). The slurry was filtered, and filter cake was washed with 10 mL of dichloromethane. The organic layers were removed under reduced pressure, and the residue was purified by column chromatography on silica gel using a gradient solvent system of 0 – 10% ethyl acetate in hexane to afford the desired compound 5. Characterization of the compound: Colorless solid (yield: 62%) ^{1}H NMR (600 MHz, $CDCl_3$) δ_{ppm} 8.17 – 8.16 (m, 1H), 7.59 – 7.58 (m, 1H), 7.53 – 7.50 (s, 1H), 6.96 (s, 2H), 6.89 – 6.86 (m, 2H), 6.62 – 6.60 (m, 2H), 5.57 (s, 2H), 5.23 (s, 2H), 4.02 (s, 2H), 2.94 (s, 12H); ^{13}C NMR (151 MHz, $CDCl_3$) δ_{ppm} 154.0, 143.0, 136.3, 130.7, 129.0, 127.0, 125.6, 122.7, 116.2, 111.8, 74.8, 73.2, 40.5, 39.9; HRMS (ESI) calcd. for $C_{25}H_{27}N_3O_4$ $[M + H]^+$: 434.2074, found: 434.2076.

Synthesis of N^2,N^2,N^{15},N^{15}-tetramethyl-7-nitro-N^2,N^{15}-dioctyl-6,11-dihydro-17H-tribenzo[c,g,j][1,6]dioxacycloundecine-2,15-diaminium (nIR8) – To a stirring solution of compound 5 was added K_2CO_3 (0.827 mmol) and the reaction mixture was continued to stir for few minutes at room temperature. After that, 1-iodooctane (1.74 mmol) was added, and the reaction mixture was heated under reflux condition for 12 hours. The progress of the reaction was monitored by TLC. After maximum consumption of compound 5, the reaction mixture was cooled down to room temperature, and unused K_2CO_3 was removed by filtration. Then organic solvent was removed under reduced pressure to yield an oily crude product. The mixture was purified through silica gel column chromatography with a solvent gradient system of 15–35% ethyl acetate in hexane to afford the pure product, **nIR8**. Characterization of compound **nIR8**: brown gummy liquid (yield: 78%) ^{1}H NMR (600 MHz, $CDCl_3$) δ_{ppm} 8.17 – 8.15 (m, 1H), 7.59 – 7.58 (m, 1H), 7.53 – 7.51 (s, 1H), 6.95 (s, 2H), 6.88 – 6.86 (m, 2H), 6.61 – 6.59 (m, 2H), 5.56 (s, 2H), 5.23 (s, 2H), 4.01 (s, 2H), 3.62 – 3.59 (m, 4H), 3.48 (s, 12H), 1.79 – 1.75 (m, 4H), 1.41 – 1.36 (m, 4H), 1.31 – 1.27 (m, 23H), 0.90 (t, 6H); ^{13}C NMR (151 MHz, $CDCl_3$) δ_{ppm} 154.0, 143.0, 136.3, 130.7, 129.0, 127.0, 125.6, 122.7, 116.2, 111.8, 74.8, 73.2, 67.3, 53.7, 40.5, 39.8, 31.9, 29.6, 29.4, 29.4, 29.3, 26.0, 23.2, 22.7, 14.1; ESI-MS (ESI+) m/z: $[(M + Na)]^+$682.4988.

Synthesis of N^2,N^{15}-didodecyl-N^2,N^2,N^{15},N^{15}-tetramethyl-7-nitro-6,11-dihydro-17H-tribenzo[c,g,j][1,6]dioxacycloundecine-2,15-diaminium (nIR12) – To a stirring solution of compound 5 was added K_2CO_3 (0.827 mmol) and the reaction mixture was continued to stir for few minutes at room temperature. After that, 1-iododododecane (1.74 mmol) was added, and the reaction mixture was heated under reflux condition for 12 hours. The progress of the reaction was monitored by TLC. After maximum consumption of compound 5, the reaction mixture was cooled down to room temperature, and unused K_2CO_3 was removed by filtration. Then organic solvent was removed under reduced pressure yielded an oily crude product. The mixture was purified through silica gel column chromatography with a solvent gradient system of 15–30% ethyl acetate in hexane to afford the pure product, **nIR12**. Characterization of compound **nIR12**: Brown gummy liquid (yield: 86%) ^{1}H NMR (600 MHz, $CDCl_3$) δ_{ppm} 8.16 – 8.14 (m, 1H), 7.58 – 7.57 (m, 1H), 7.52 – 7.51 (s, 1H), 6.94 – 6.93 (m, 2H), 6.86 – 6.85 (m, 2H), 6.60 – 6.58 (m, 2H), 5.55 (s, 2H), 5.22 (s, 2H), 4.00 (s, 2H), 3.62 – 3.59 (m, 4H), 3.47 (s, 12H), 1.78 – 1.75 (m, 4H), 1.40 – 1.38 (m, 4H), 1.31 – 1.26 (m, 23H), 0.89 (t, 6H); ^{13}C NMR (151 MHz, $CDCl_3$) δ_{ppm} 150.0, 143.0, 136.3, 130.7, 129.0, 127.0, 125.6, 122.7, 116.2, 111.8, 74.8, 73.2, 67.3, 53.7, 40.5, 39.8, 31.9, 29.6, 29.4, 29.4, 29.3, 26.0, 23.2, 22.7, 14.1; ESI-MS (ESI+) m/z: $[(M + 2HCOO^-)]^+$ 861.5770.

Synthesis of N^2,N^{15}-dihexadecyl-N^2,N^2,N^{15},N^{15}-tetramethyl-7-nitro-6,11-dihydro-17H-tribenzo[c,g,j][1,6]dioxacycloundecine-2,15-diaminium (nIR16) – To a stirring solution of compound 5 was added K_2CO_3 (0.827 mmol) and the reaction mixture was continued to stir for few minutes at room temperature. After that, 1-iodohexadecane (1.74 mmol) was added, and the reaction mixture was heated under reflux condition for 12 hours. The progress of the reaction was monitored by TLC. After maximum consumption of compound 5, the reaction mixture was cooled down to room temperature, and unused K_2CO_3 was removed by filtration. Then organic solvent was removed under reduced pressure yielded an oily crude product. The mixture was purified through silica gel column chromatography with a solvent gradient system of 15–30% ethyl acetate in hexane to afford the pure product as a brown gummy liquid, **nIR16**. Characterization of compound **nIR16**: Brown gummy liquid (yield: 83%) ^{1}H NMR (600 MHz, $CDCl_3$) δ_{ppm} 8.15 – 8.13 (m, 1H), 7.58 – 7.56 (m, 1H), 7.51 – 7.49 (s, 1H), 6.95 – 6.91 (m, 2H), 6.85 – 6.84 (m, 2H), 6.59 – 6.58 (m, 2H), 5.54 (s, 2H), 5.21 (s, 2H), 3.99 (s, 2H), 3.59 – 3.56 (m, 4H), 3.45 (s, 12H), 1.80 – 1.75 (m, 4H), 1.42 – 1.38 (m, 4H), 1.30 – 1.26 (m, 23H), 0.88 (t, 6H); ^{13}C NMR (151 MHz, $CDCl_3$) δ_{ppm} 154.0, 143.0, 136.3, 130.8, 129.0, 127.1, 125.6, 122.7, 116.2, 111.8, 74.7, 73.2, 67.3, 53.9, 49.4, 40.5, 39.8, 31.9, 29.7, 29.6, 29.5, 29.4, 29.3, 26.1, 23.2, 22.7, 14.1; ESI-MS (ESI+) m/z: $[M]^+$ 884.6773.

Purity analysis of the lipids – The purity of the synthesized compounds was analyzed by analytical HPLC using Agilent 1260 Infinity II HPLC system with an Ascentis® express C18, 15 cm × 4.6 mm, 2.7 µm HPLC column. Acetonitrile/water gradient was used as the mobile phase at a flow rate of 0.5 mL/minute for 25 minutes run time. The spectra were recorded using a UV-detector at 254 nm.

III. preparation of soluble aggregates

The compounds were dried under reduced pressure for 3 hours to prepare thin films. After that, 500 µL of 20 mM HEPES buffer, pH 7.2, containing 100 mM KCl, was added into the thin film and heated to 30-40 °C for 10 min. The solution was then vortexed well to mix the thin film. Finally, the solution was sonicated more than ten times with 30 s of sonication followed by 30 s of cooling on ice cycles. A hand-held mini extruder (Avanti Polar Lipids, Alabaster, AL) with polycarbonate membrane (diameter of 200 nm) was used to prepare small soluble aggregates at room temperature.

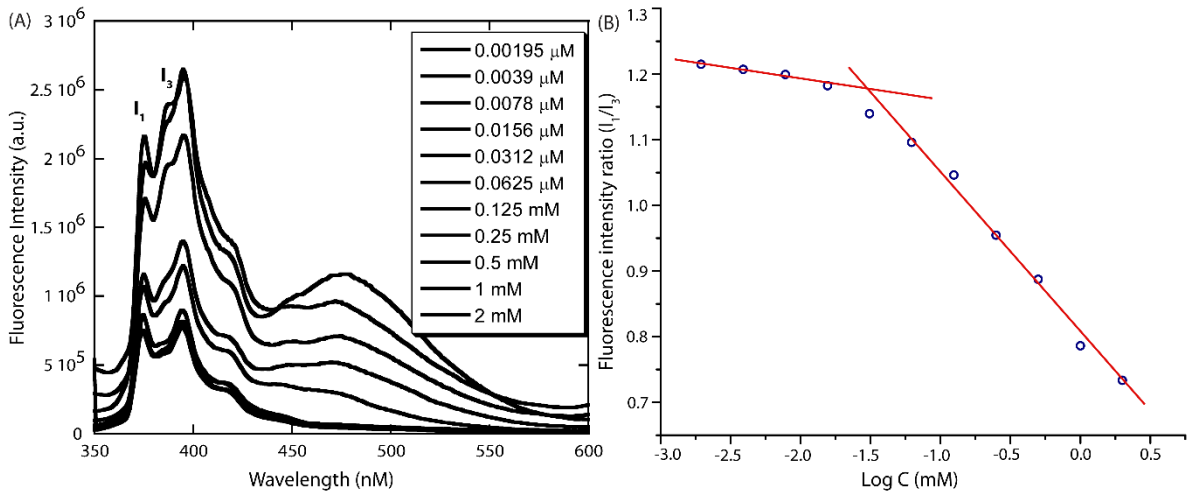

Fig. S1. Measurement of critical aggregation constant of **nIR12** using pyrene probe. The plot of pyrene fluorescence against increasing concentration of **nIR12** (A). Variation of I_1/I_3 fluorescence intensity against increasing concentration of **nIR12** (B).

IV. Transmission electron microscopy

The morphology of the aqueous soluble aggregates of the amphiphile was investigated both in the presence and absence of NIR (808 nm, 1 W cm^{-2} for 10 min.) light by transmission electron microscope (TEM).[2, 3] First, the aqueous solution of the compound was prepared by the above-mentioned method in 20 mM HEPES buffer, pH 7.2, containing 100 mM KCl. A 10 µL of the solution was placed onto a carbon-coated copper grid and allowed to settle down for 1 minute. The grid was then carefully blotted with filter paper, and only a trace amount of the solution in the middle of the grid was kept. After that, the grid was allowed to dry for 10 minutes at 30 °C. Finally, 10 µL of 2% uranyl acetate solution (in

water) was added to the grid and allowed to dry for another 1 min at room temperature. The excess uranyl acetate solution was soaked off with tissue paper, and the grid was dried overnight at 30 °C. The images were collected using JEOL JEM 2100 transmission electron microscope (operated at a maximum accelerating voltage of 200 kV).

V. Phase transition temperature measurements

To determine the phase transition temperature (T_m) of the aqueous soluble nanoaggregates, the temperature-dependent steady-state anisotropy measurements were performed.[2, 3] The environment-sensitive dye 1, 6 -diphenyl-1, 3, 5-hexatriene (DPH) was used as the fluorescence probe to measure the change in anisotropy values. The soluble aggregates were prepared according to the method described in the previous section (the hydration was done by using 20 mM HEPES buffer, pH 7.2, containing 100 mM KCl). After that, the solution of compound (1000 µL) and DPH solution (10 µL of 1 mM stock solution in THF) was taken in a microcentrifuge tube (final concentration of DPH was 10 µM; DPH < 1% v/v in compound solution). The solution was kept at room temperature under tumbling conditions for overnight to ensure the maximum incorporation of DPH molecules inside the hydrophobic core of the soluble aggregates. Then steady-state fluorescence anisotropy measurements were performed with a refrigerated system using a Peltier temperature controller connected to a Fluoromax-4 spectrofluorometric (Horiba Scientific). The degree (r) of anisotropy in the DPH fluorescence (λ_{ex} = 350 nm; λ_{em} = 429 nm) was calculated using the following equation (eq. 1) at the peak of the fluorescence spectrum. The I_{VV} and I_{VH} are the fluorescence intensities of the emitted light polarized parallel and perpendicular to the excited light, respectively, and $G = I_{VH}/I_{HH}$ is the instrumental grating factor.

$$r = \frac{(IVV - GIVH)}{(IVV + 2GIVH)} \quad \text{.....Eq. 1}$$

At every 3-4 °C temperature difference, the anisotropy values were recorded, apart from the near to the T_m value; in that case, the anisotropy values were collected at every 1 or 2 °C. All anisotropy values of the DPH probe are the mean values of three individual measurements. Finally, to determine the T_m value of the compound, plots of the degree of anisotropy (r) of the DPH probe as a function of temperature were investigated.

VI. pH-dependent particle size and surface charge of the soluble aggregates

The soluble aggregates were prepared according to the method as described in the earlier section in 25 mM HEPES buffer, pH 7.2, containing 100 mM KCl.[2, 3] Different buffer solutions were freshly prepared using isosmotic buffers consisting of 10 mM buffering agent and 10 mM salt to vary the pH range (pH 3

to pH 9.0) and used for the measurements. Citric acid and trisodium-citrate for pH 3.0–6.5; 3-(N-morpholino)propanesulfonic acid (MOPS) for pH 7.0 and tris(hydroxymethyl)aminomethane (Tris)–HCl were used for pH 7.5–8.5. Both the zeta potential and hydrodynamic diameter of the soluble aggregates at different pH were measured using a Zetasizer Nano ZS90 (Malvern, Westborough, MA) instrument at 25 °C.

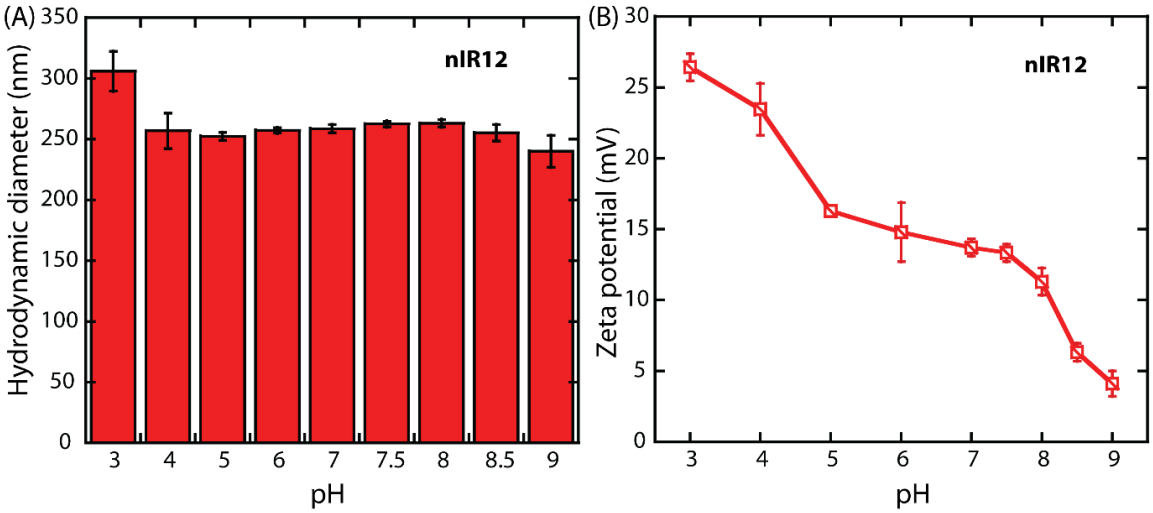

Fig. S2. Variation of hydrodynamic diameter (A) and zeta potential (B) of the soluble aggregates of **nIR12** at various pH.

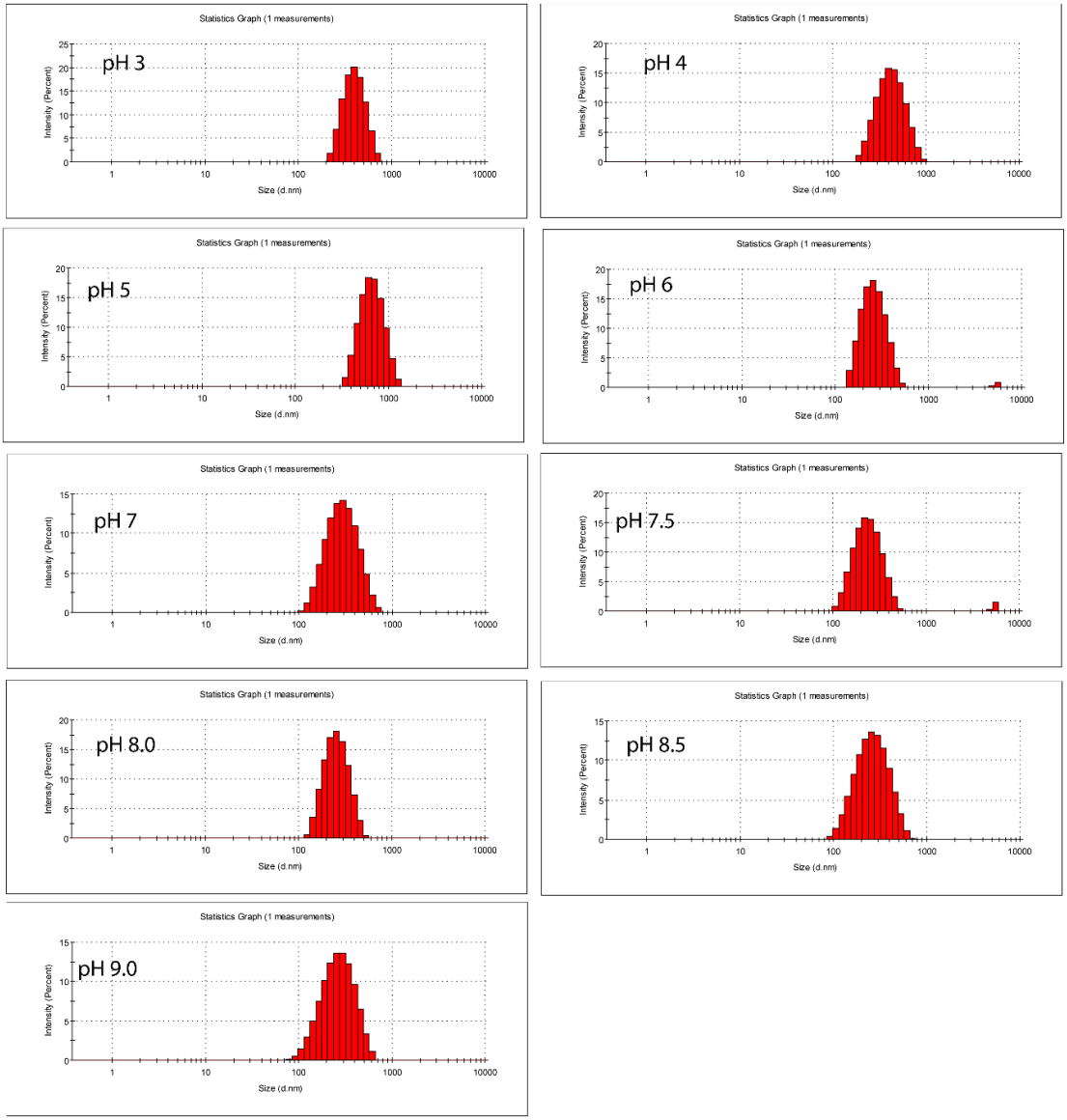

Fig. S3. Dynamic light scattering (DLS) measurements of **nIR12**. The size distribution of the extruded soluble aggregates generated from **nIR12** (measured at 25 °C). Content is given in percentage distribution of different sized soluble aggregates at different pH.

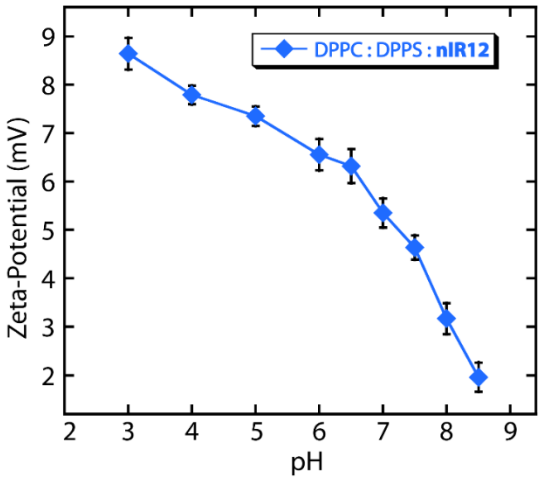

Fig. S4. Variation of zeta potential of the lipid mixture DPPC/DPPS/**nIR12** (2:2:1) at various pH.

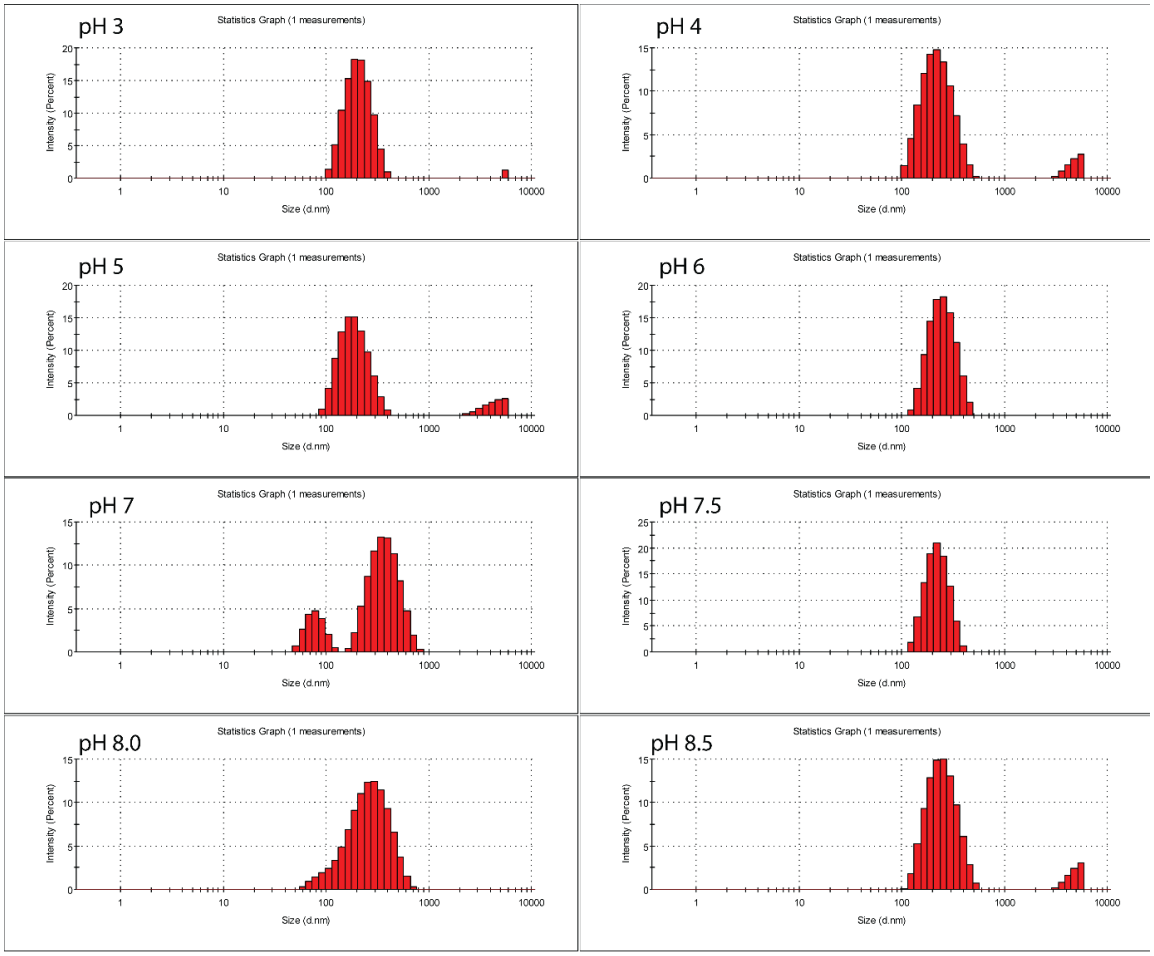

Fig. S5. Dynamic light scattering (DLS) measurements for lipid mixture of DPPC/DPPS/**nIR12** (molar ratio 2:2:1). The size distribution of the extruded soluble aggregates generated from the lipid mixture of DPPC/DPPS/**nIR12** (measured at 25 °C). Content is given in percentage distribution of different sized soluble aggregates at different pH.

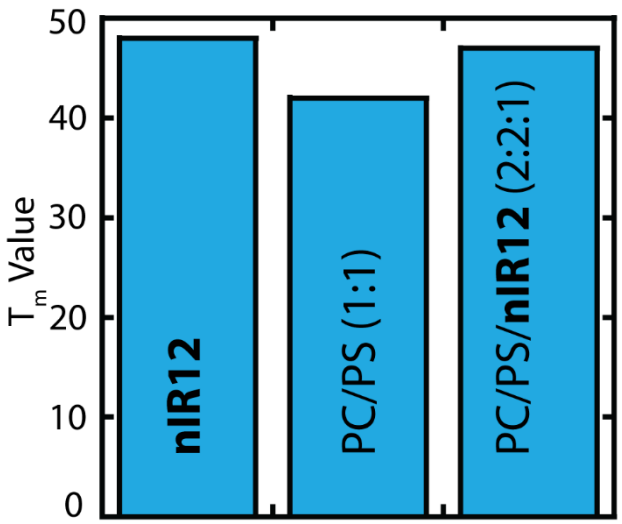

Fig. S6. The temperature-dependent fluorescence anisotropy measurement of environment-sensitive 1,6-diphenyl-1,3,5-hexatriene dye incorporated within the aqueous soluble aggregates.

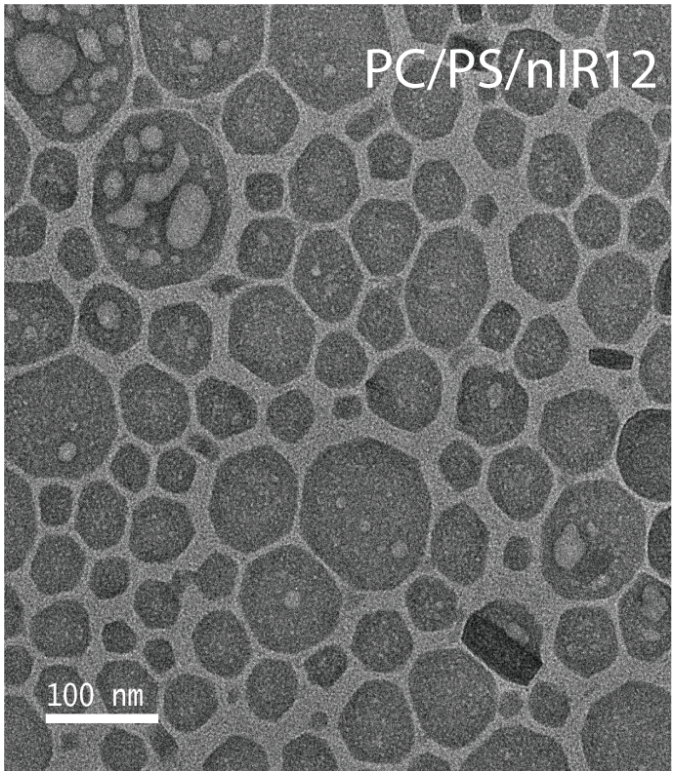

Fig. S7. Representative FETEM image of the water-soluble aggregates produced from lipid mixture of DPPC/DPPS/**nIR12** (2:2:1).

VII. Molecular dynamics simulation studies

CHARMM-GUI was used to create the 1-palmitoyl-2-oleoyl-sn-glycero-3-phosphocholine (POPC) and palmitoyl-oleoyl phosphatidylserine (POPS) bilayer-membrane.[4] Generalized Amber Force Field (gaff)

was used to model the molecule, sodium, and chloride ions.[5] CHARMM36 force field was used to model the bilayer-membrane, while TIP3P was used for water molecules.[6] We modeled the interaction of the molecules with the lipid bilayer membrane by all atom molecular dynamics (MD) simulations as implemented in the NAMD package.[7, 8] Particle-mesh Ewald (PME) method was used in order to take care of the long-range interaction.[9] Van der Waals cut-off was set at 10 Å. Periodic boundary conditions were used, and SHAKE algorithm was used in order to constrain the covalent hydrogen atoms.[10] The systems were modeled in NPT ensembles at T = 300 K, and the time step was 1fs. The Langevin damping was used to thermalize the systems while the damping coefficient γ is 1 ps^{-1}.

In order to investigate the interaction of the lipid molecule with the membrane, first, we solvated the bilayer-membrane into a water box. Then we placed one lipid molecule on top of the membrane layer. Initially, we minimized the system for 20,000 steps while the lipid molecule was held fixed. After that, we equilibrated the system for 5 ns at 300 K where the molecule was held fixed. Then systems were equilibrated for ~100 ns at 300 K where all the atoms were released. The simulated system contains 70 POPC lipid molecules, 70 POPS lipid molecules, one lipid molecule. Sodium and chloride ions were added to maintain the 150 mmol salt concentration. The size of the simulated box was 77 x 77 x 120 $Å^3$. The total atom number is 43002. The MD simulation was performed for 100 ns.

We observed that the oxygen (which are in the ring) and amine-nitrogen atoms of the lipid molecule interacted with the oxygen atoms and phosphate atoms of the lipid-membrane molecule. After another 5 ns, the hydrophobic part (one tail) of the molecule started to enter into the membrane as shown in Fig. S6. Eventually, after another 15 ns, both the hydrophobic tails entered into the membrane, where the head part remained outside of the membrane. This could be due to the insertion of the hydrophobic part of the lipid molecules into the membrane to have superior hydrophobic-hydrophobic interactions, were as the head part would like to interact more with water as well ions that were out of the membrane.

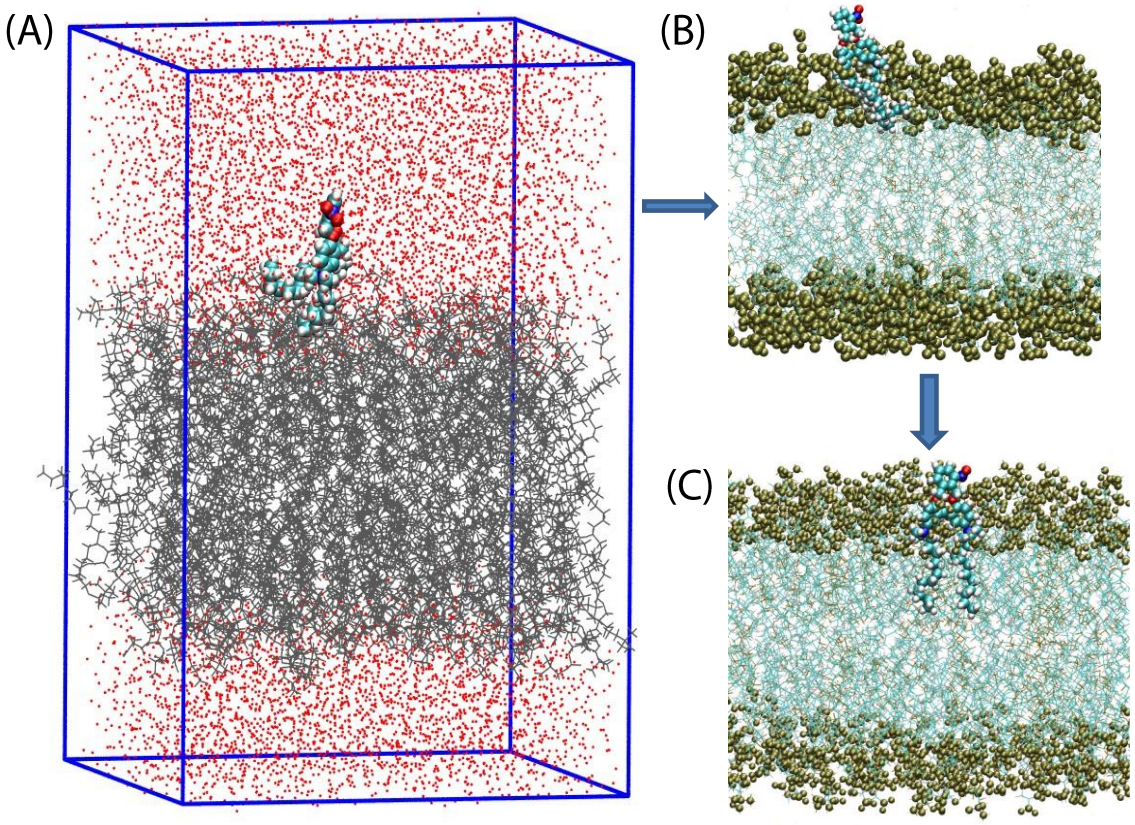

Fig. S8. Lipid insertion into membrane bilayer. The simulated system consists of DOPC, DOPS lipids and one molecule of compound **nIR12**, and water molecules (A). After 7 ns one hydrophobic chain started to enter inside (B). After another 15 ns both chains were into the membrane (C).

VIII. NIR light-induced cleavage of the amphiphile

We monitored the light cleavage ability of the compound with the help of NMR. The compound **nIR12** was dissolved in $CDCl_3$, and a NIR laser diode (808 nm) of power density (1 W cm^{-2}) was set at 3 cm above the liquid surface and irradiated for 2, 3, 5, 7, 10 minutes, and the NMR spectra were recorded of corresponding time. The cleavage of **nIR12** was also analyzed in mass spectrometry.

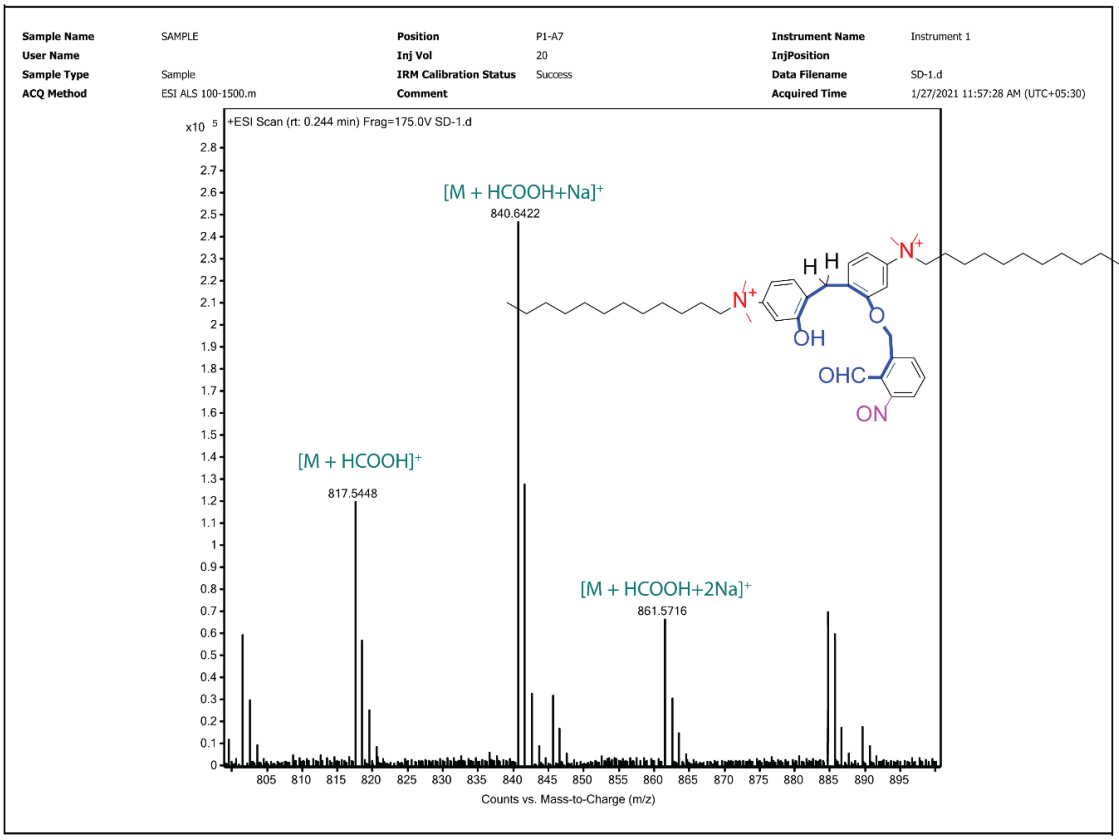

Fig. S9. HRMS analysis of NIR light-mediated photocleavage of **nIR12**.

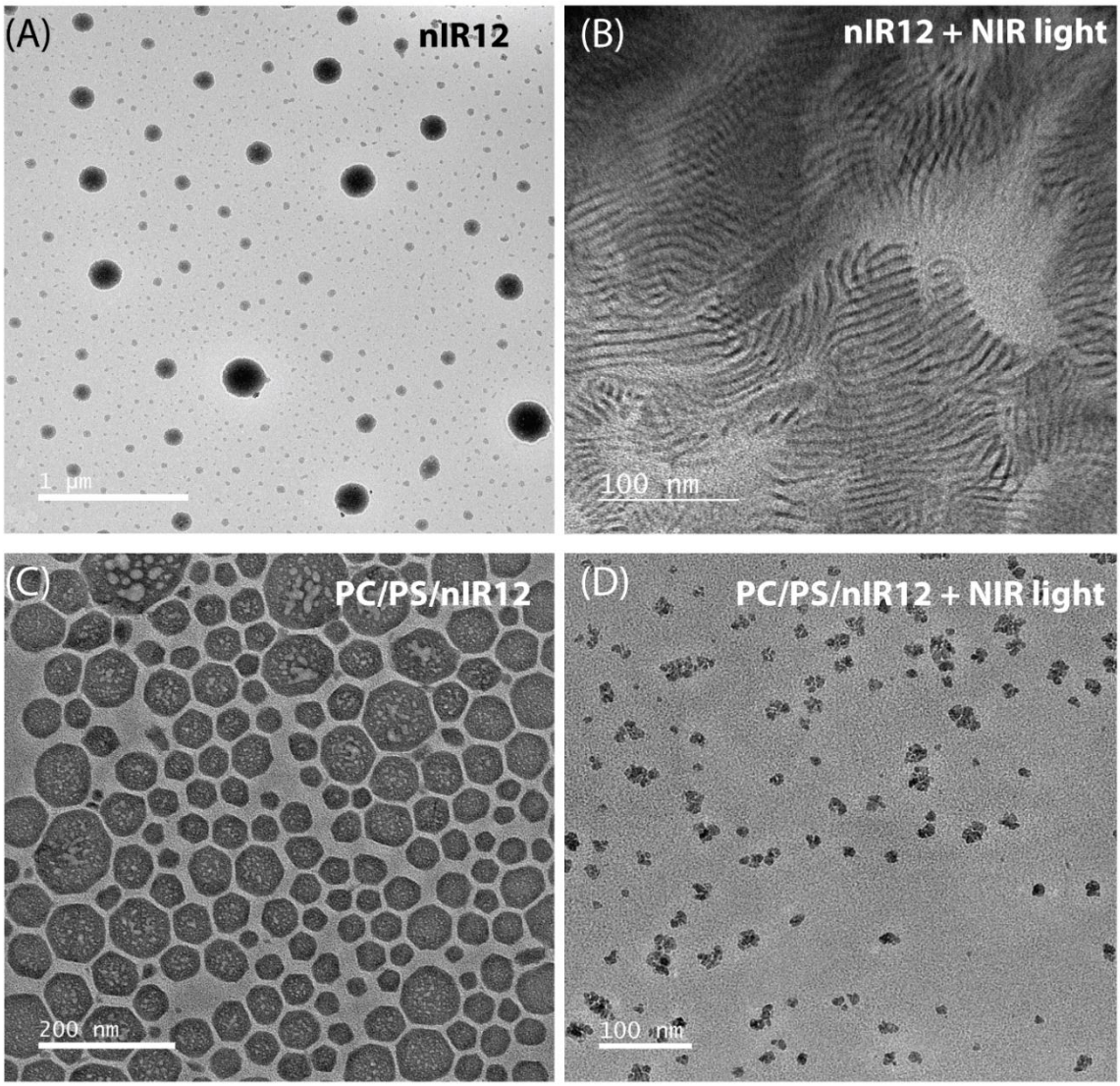

Fig. S10. Representative FETEM image of the water-soluble aggregates produced from only **nIR12** before (A) and after (B) NIR-light treatment (808 nm, 1 W cm^{-2}; 10 min.). Representative FETEM image of the lipid mixture produced from DPPC/DPPS/**nIR12** before (C) and after (D) NIR-light treatment (808 nm, 1 W cm^{-2}; 10 min.).

IX. Doxorubicin encapsulation and release efficiency measurement

The DOX release profiles from vesicles were determined using dialysis-based method according to the reported procedure.[11] Vesicles containing DOX (1 mM DOX in 50 mM of lipid in HEPES buffer) were added into a D-Tube™ Dialyzer (Millipore Sigma, molecular weight cut-off 10 kD). Tubes were sealed and placed into a reservoir loaded with 10 mL of the same buffer. At scheduled time points, 20 µL of the reservoir solution was injected through analytical HPLC (C18, 15 cm × 4.6 mm, 2.7 µm) to monitor the release of free DOX. Concentrations of released DOX in the supernatant were determined by measuring area of the chromatogram at 254 nm. Acetonitrile and water were used as mobile phase with flow rate of

0.5 mL/minute. To measure the loaded drug, the DOX@**nIR12** and DOX@(PC/PS/**nIR12**) was dissolved in acetonitrile and recorded through HPLC.

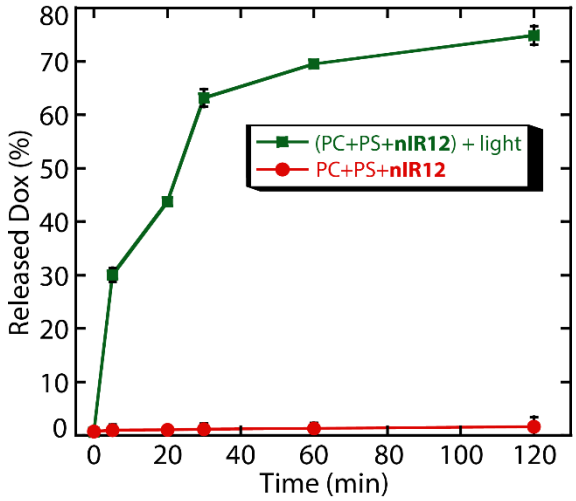

Fig. S11. The Dox release profile of DPPC/DPPS/**nIR12** (2:2:1) at pH 7.4 without and with NIR-light treatment (10 min).

X. Cell culture

The MDA-MB-231 cells were cultured in Dulbecco's Modified Eagle Medium (DMEM, GIBCO) supplemented with 10% fetal bovine serum (FBS, GIBCO) and penicillin-streptomycin solution (GIBCO; 100 U/ml penicillin and 100 µg/ml streptomycin).[2, 3] PBMC (Peripheral Blood Mononuclear Cell) were isolated from the blood sample of a healthy donor and cultured in DMEM supplemented with the above-mentioned media. Cells were maintained in a humidified atmosphere of 5% CO_2 at 37 °C in a CO_2 incubator. In all experiments, the medium was changed daily with complete media.

XI. Determination of cell viability using MTT assay

The MDA-MB-231 and PBMC cells were cultured, as mentioned earlier.[2, 3] For the cell viability study, both the cell lines were seeded in 96-well flat-bottomed plates at a density of 2×10^4 cells per well and incubated for 24 hours in complete media in a CO_2 incubator. Thereafter, cells were treated with different concentrations of **nIR12**, free Dox, and Dox@**nIR12** (in the presence and absence of 808 nm light according to the experiment) for additional 48 hours. The cell viability was then assessed using MTT [3-(4,5-dimethylthiazol-2-yl)-2,5-diphenyl-2H-tetrazolium bromide] (Sigma-Aldrich) assays. Briefly, media was discarded, and cells were treated with MTT (final concentration: 0.5 mg/ml) for 2 hours at 37 °C in a CO_2 incubator, and the resulting purple-colored formazan crystals were dissolved in 200 µL of DMSO. Cell viability was then measured using Multiscan GO (Thermo Scientific) at 570 nm. Cell viability (%) = (absorbance intensity (sample)) / (absorbance intensity (control)) × 100%.

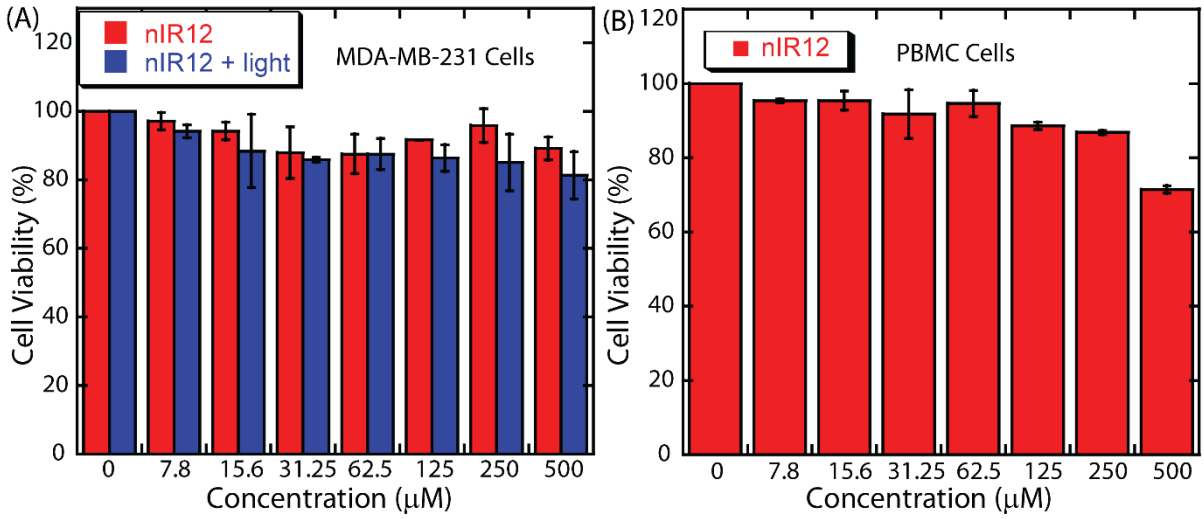

Fig. S12. Viabilities of MDA-MB-231 (A) and PBMC (B) cells in the presence of **nIR12** (in the absence and presence of NIR light) at different concentrations.

XII. Determination of cellular uptake efficiency using flow cytometry

The MDA-MB-231 cells were cultured, as mentioned earlier.[2, 3] Cells were seeded in 6-well plates at a density of 2 ×10^5 cells per well and incubated for 24 hours in complete media. The cells were then treated with different entities (Dox, Dox@**nIR12**) in the absence and presence of NIR light (808 nm, 1 W cm^{-2}, 10 min.) in 1% FBS containing media for 8 hours at 37 °C. Next, the cells were washed twice with PBS (GIBCO), trypsinized (0.05%; GIBCO) for 2 minutes at 37 °C followed by 5 min centrifugation at 800 rpm at 4°C. The supernatant was discarded, and cell pellets were re-suspended in 300 µL of PBS (supplemented with 2% FBS). Finally, the solutions were kept on ice, and the drug uptake by the MDA-MB-321 cells was analyzed by flow cytometry analysis using BD FACS Calibur Flow Cytometer (BD Biosciences). Data analysis was performed by the FCS Express 5 Flow Cytometry software.

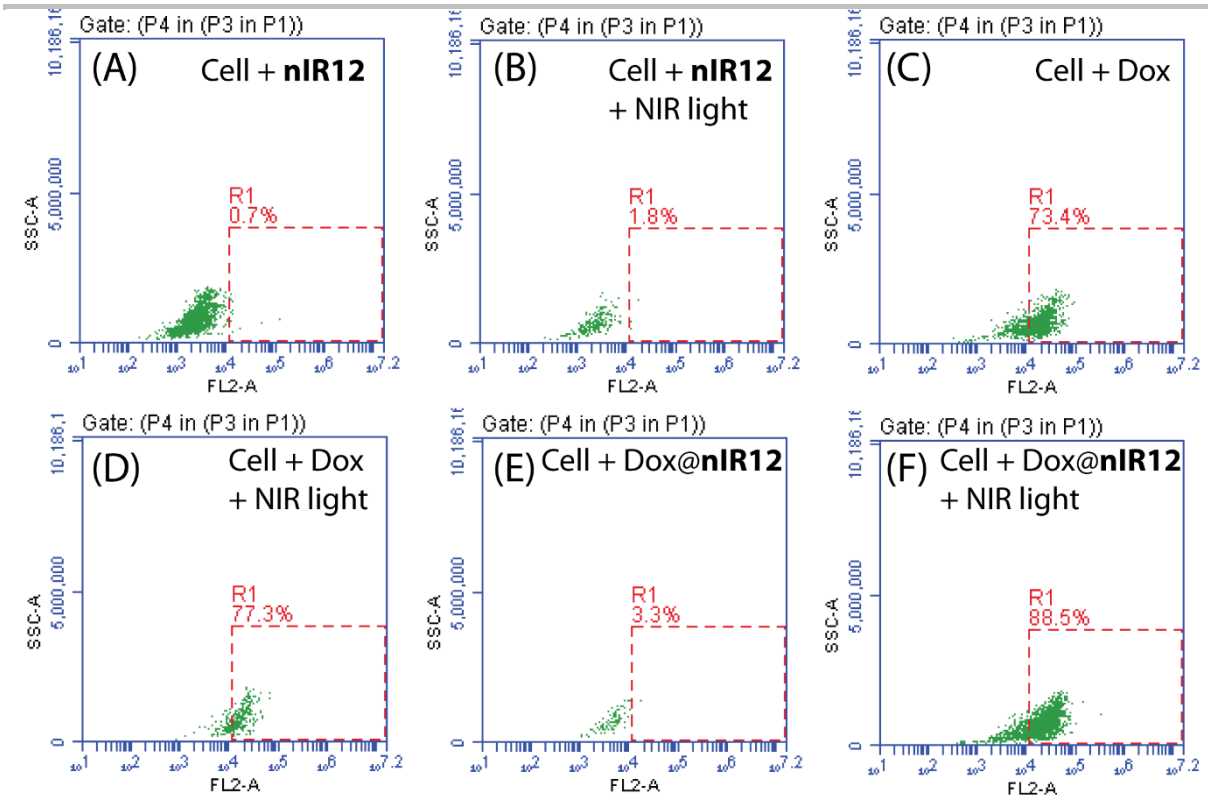

Fig. S13. Flow cytometry analysis to measure the Dox uptake efficiencies of MDA-MB-231 cells treated with free Dox (125 µM) and Dox@**nIR12** (1.25 µM of Dox and 125 µM of amphiphile) in the absence and presence of NIR light (808 nm, 1 W cm^{-2}, 10 min.). The inherent fluorescence property of Dox molecules was used for the measurement (FL2-A channel). Only cells were used as control. Cell + **nIR12** (A); Cell + **nIR12** + NIR light (B); Cell + Dox (C); (Cell + Dox) + NIR light (D); Cell + Dox@**nIR12** (E); Cell+ Dox@**nIR12** + NIR light (F).

XIII. Determination of cellular uptake using microscopy analysis

The MDA-MB-231 cells were cultured, as mentioned earlier.[2, 3] For microscopy analysis, cells were seeded in 6-well plates at a density of 1.5 $\times 10^5$ cells per well, each well containing a sterile 22 mm square coverslip (pre-coated with 0.1% gelatin) in the bottom and incubated overnight in complete media in a CO_2 incubator. Cells were then treated with Dox@**nIR12** in the presence and absence of light for 10 minutes and further incubated for 8 hours in 1% FBS containing media. Post-treatment, cells were washed with PBS buffer and fixed with 4% formaldehyde at 37 °C for 10 minutes. Coverslips were then washed thrice with PBS and treated with 0.1% Triton X-100 for 5 minutes at 37 °C. Cells were again washed thrice with PBS buffer. To counterstain the nuclei, DAPI (5 µg/mL) was added and incubated for 5 minutes. Cells were then washed thrice with PBS. Subsequently, coverslips were taken out from the wells and mounted over a glass slide. The slides were then allowed to dry for 15 mins. Finally, the microscopic analysis was performed using a confocal laser scanning microscope (CLSM; Leica TCS SP8; λ_{ex} = 488 nm, λ_{em} = 560–630 nm for Dox and λ_{ex} = 405 nm, λ_{em} = 440–480 nm for DAPI).

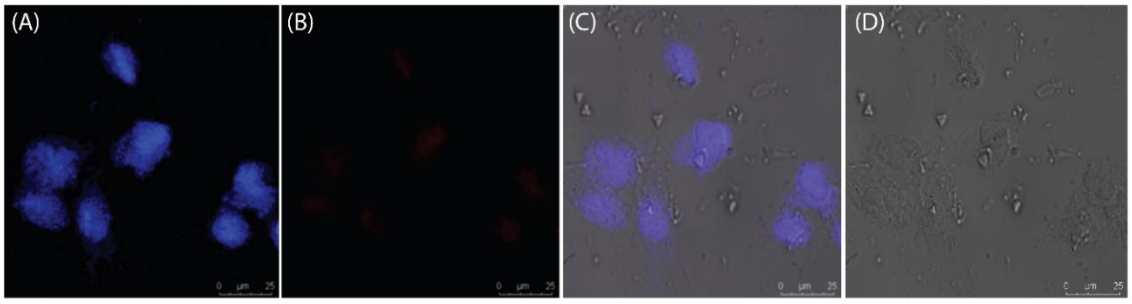

Fig. S14. Representative CLSM images of the MDA-MB-231 cells incubated with Dox@**nIR12** (1.25 µM of Dox and 125 µM of amphiphile) for 8 h (without any NIR-light irradiation). The blue channel (DAPI; A), red channel (Dox; B), overlay of the blue and red channels (C), and bright-field (D) illustrate the Dox release efficacy to MDA-MB-231 cells (without NIR–light treatment). Scale bar 25 µm.

XIV. ^{1}H NMR and ^{13}C NMR, HRMS spectra and HPLC traces of the synthesized compounds

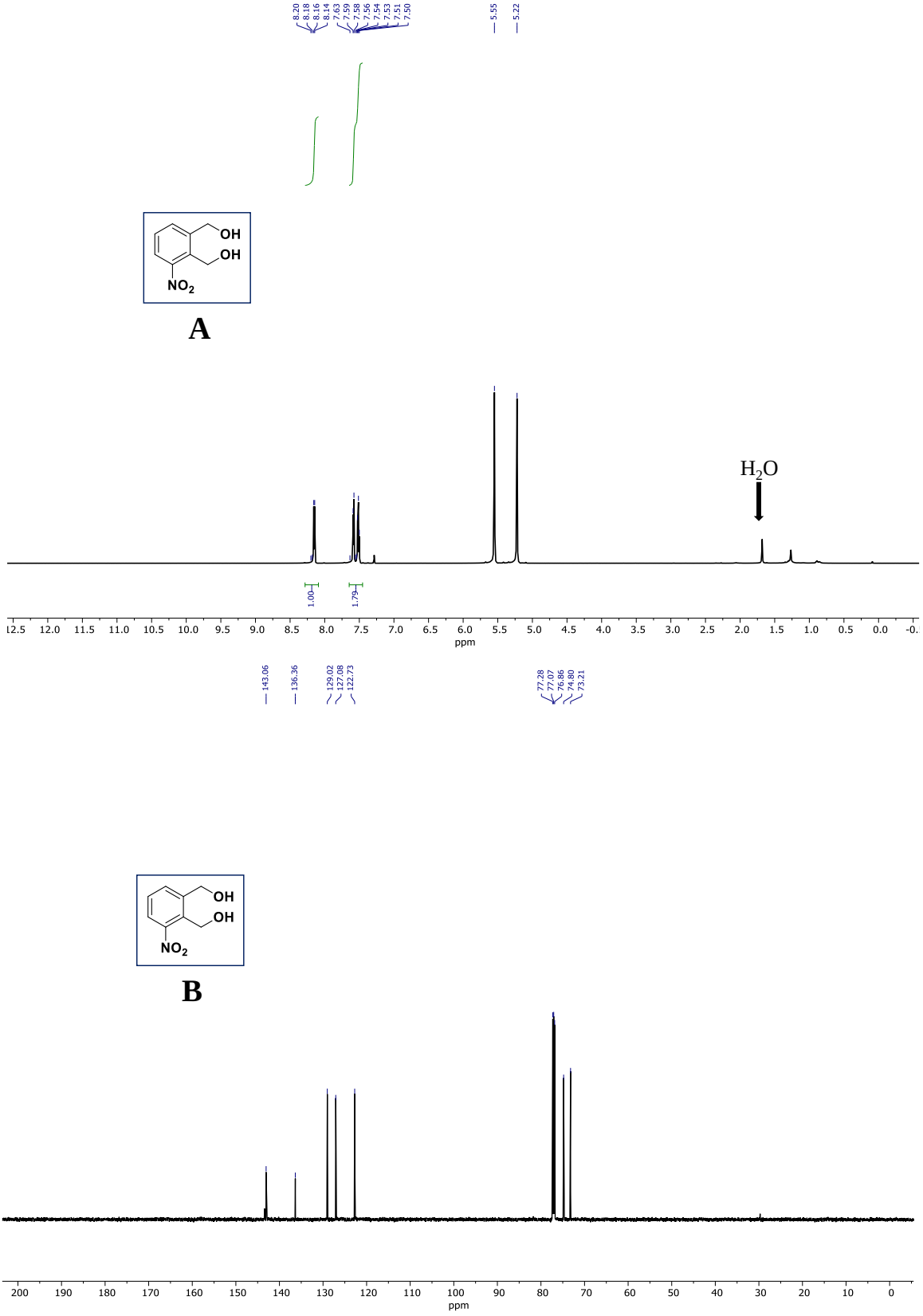

Fig. S15. ^{1}H NMR (A) and ^{13}C NMR (B) spectra of compound **4**.

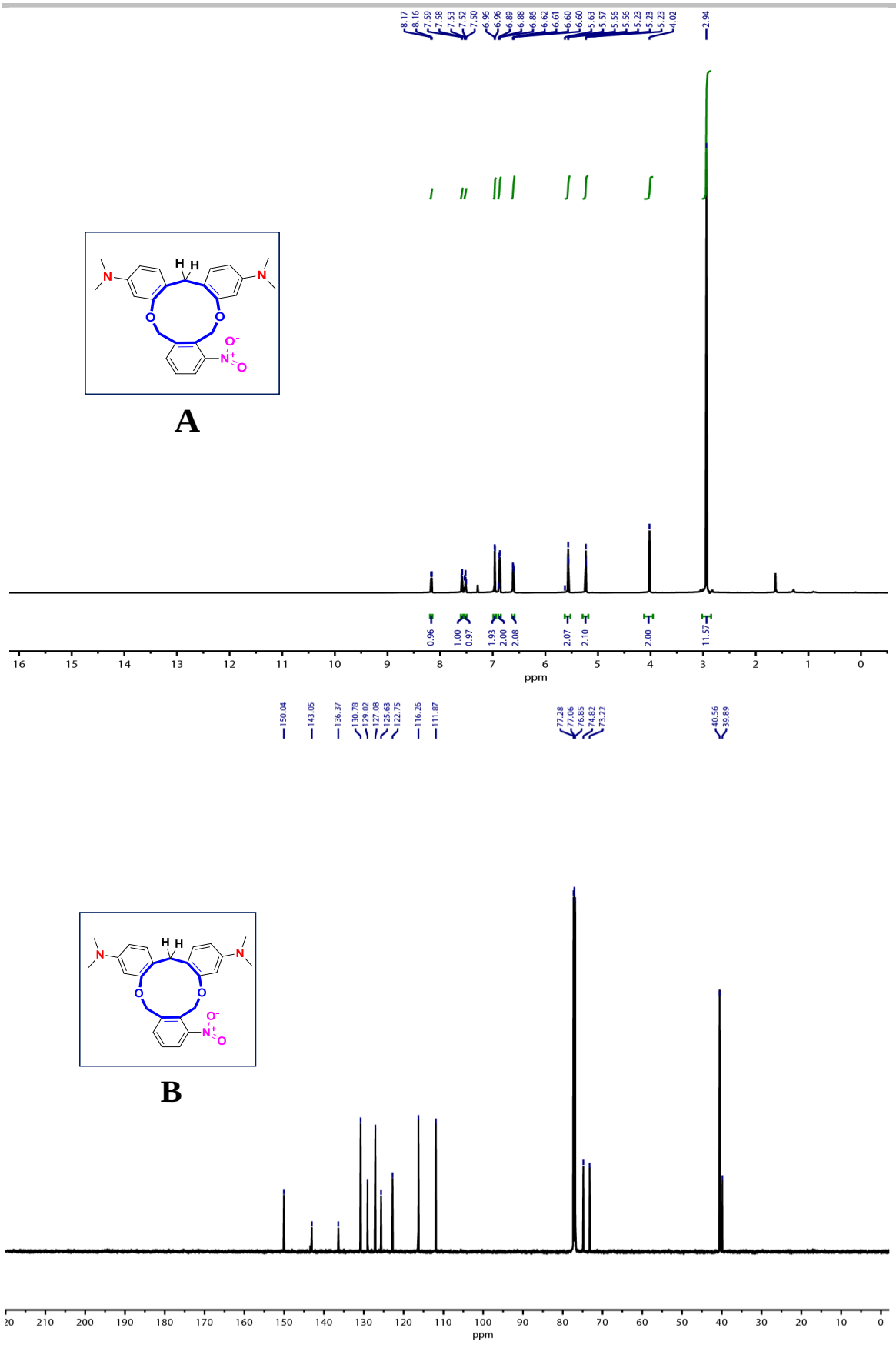

Fig. S16. ^{1}H NMR (A) and ^{13}C NMR (B) spectra of compound **5**.

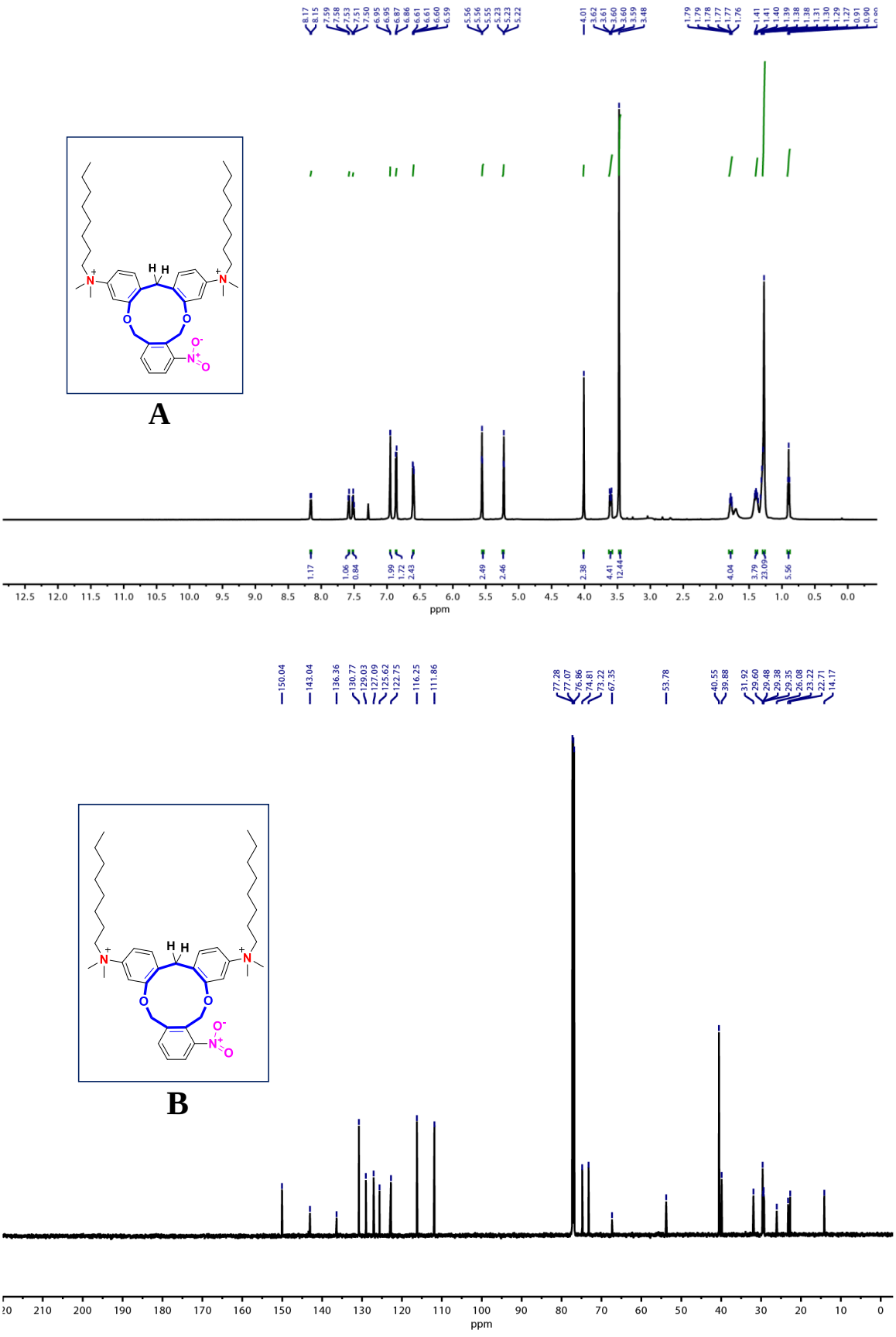

Fig. S17. ^{1}H NMR (A) and ^{13}C NMR (B) spectra of compound **nIR8**.

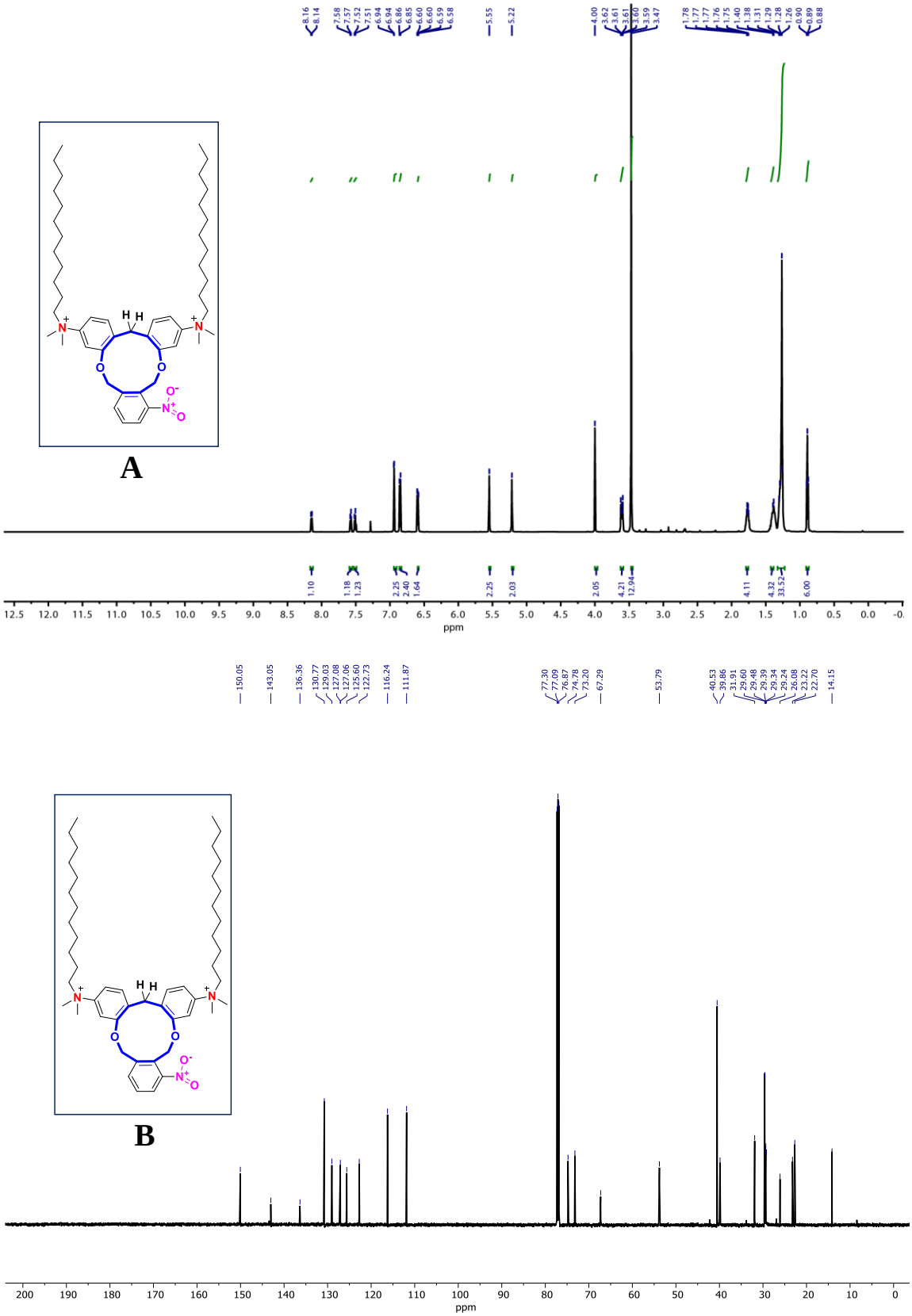

Fig. S18. ^{1}H NMR (A) and ^{13}C NMR (B) spectra of compound **nIR12**.

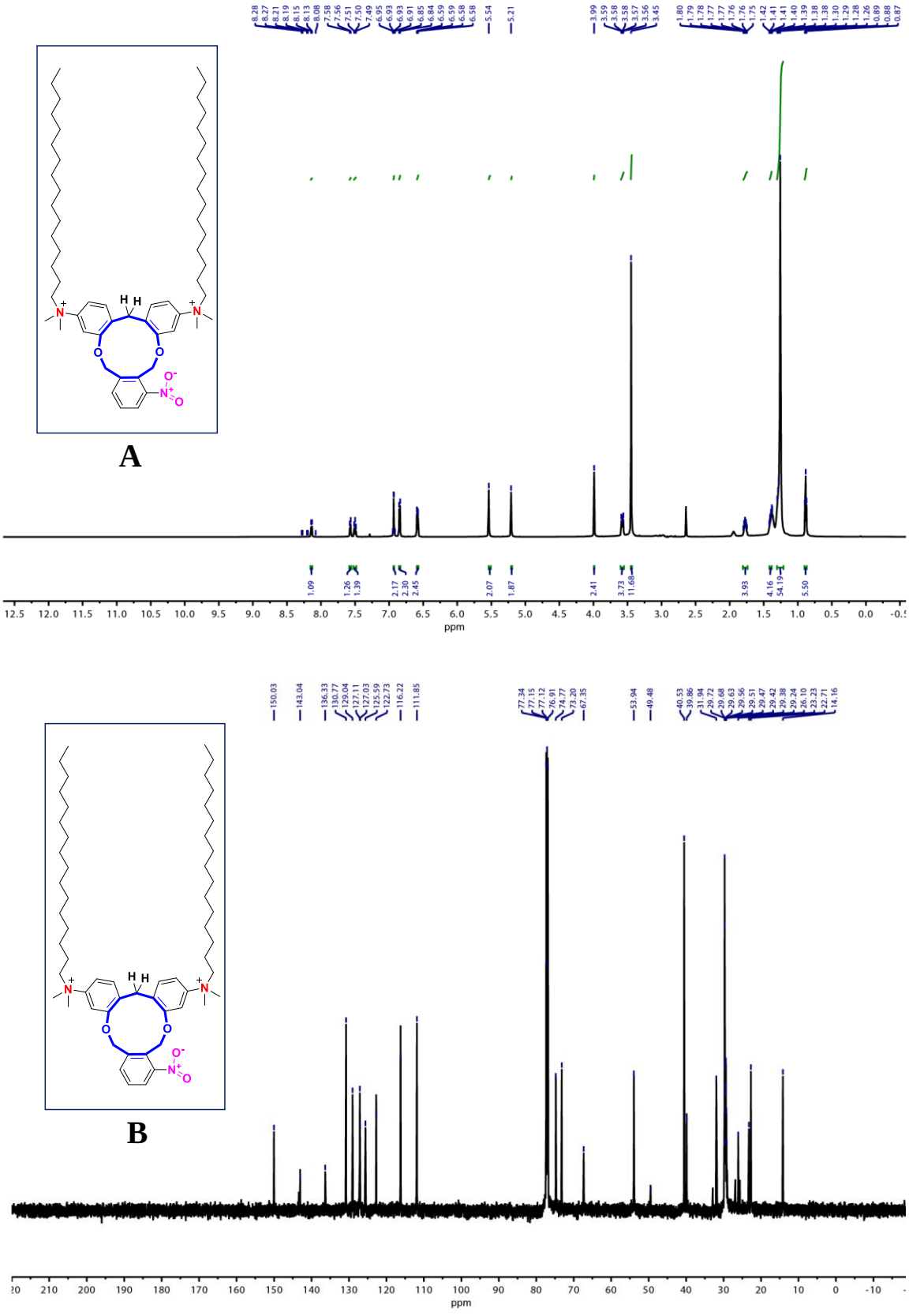

Fig. S19. ^{1}H NMR (A) and ^{13}C NMR (B) spectra of compound **nIR16**.

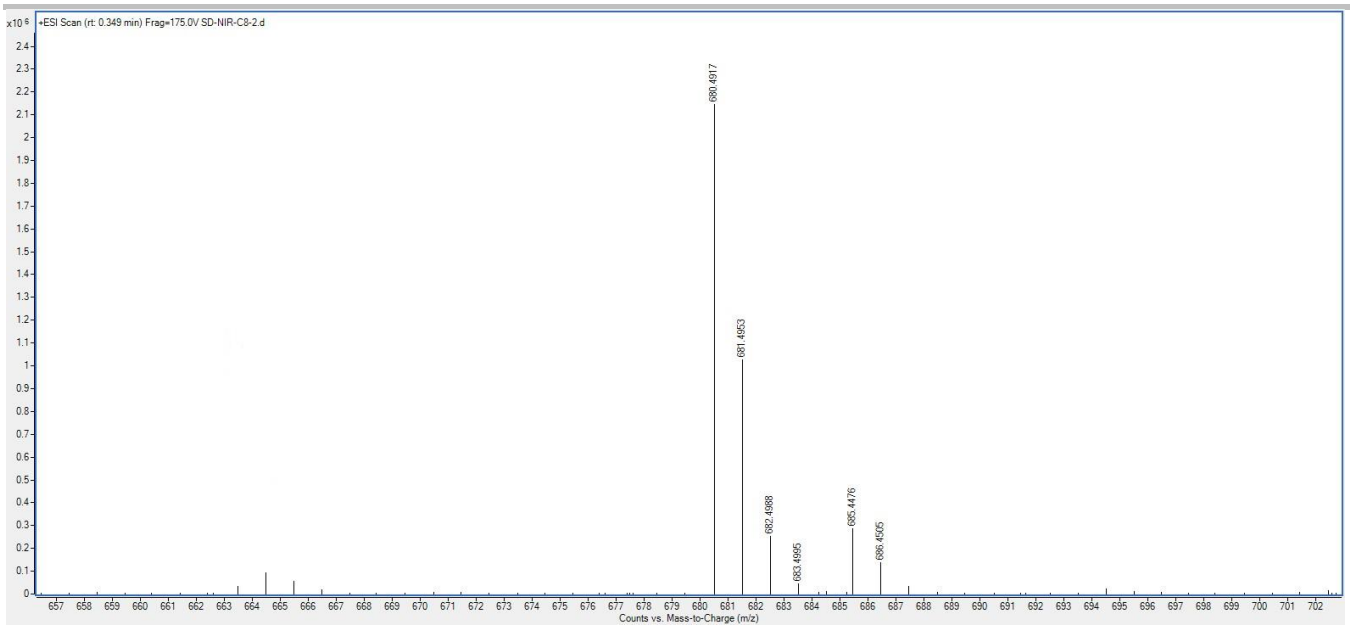

Fig. S20. ESI-MS spectra of compound **nIR8**.

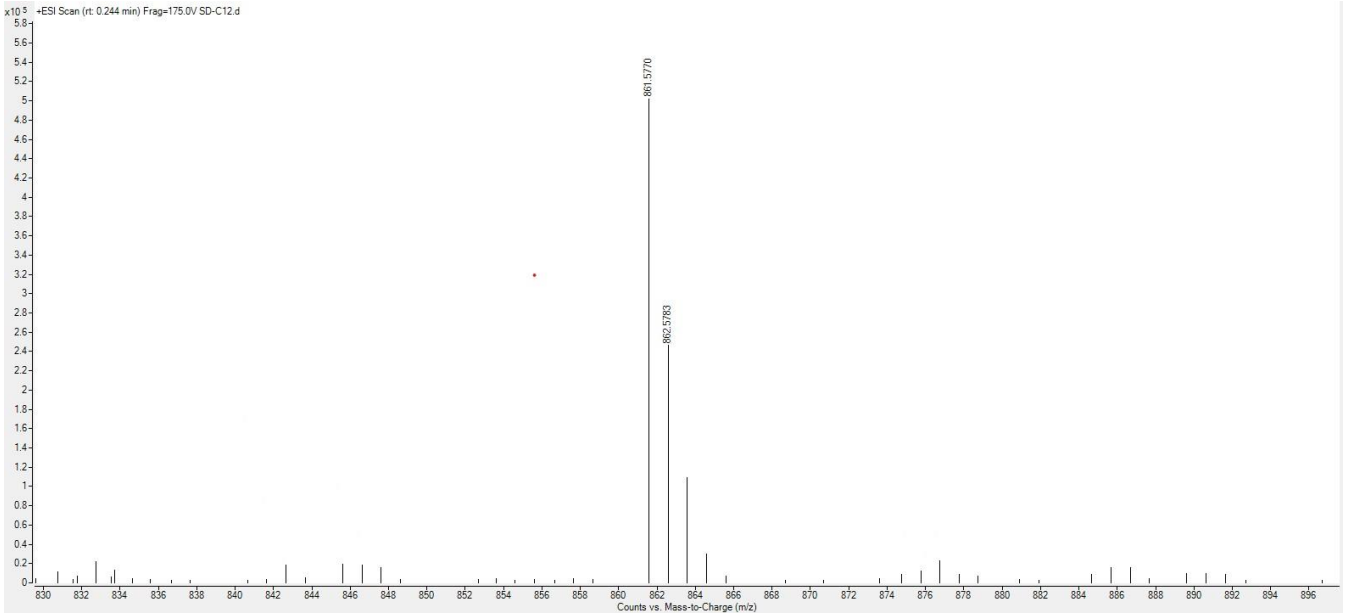

Fig. S21. ESI-MS spectra of compound **nIR12**.

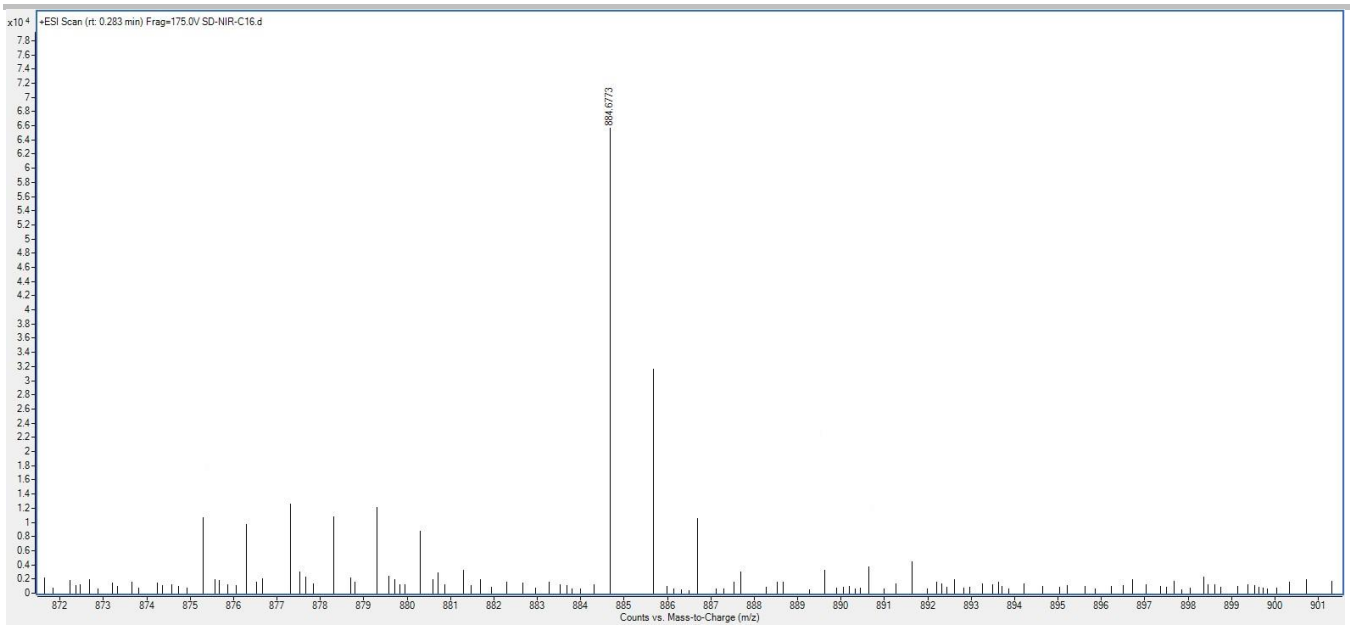

Fig. S22. ESI-MS spectra of compound **nIR16**.

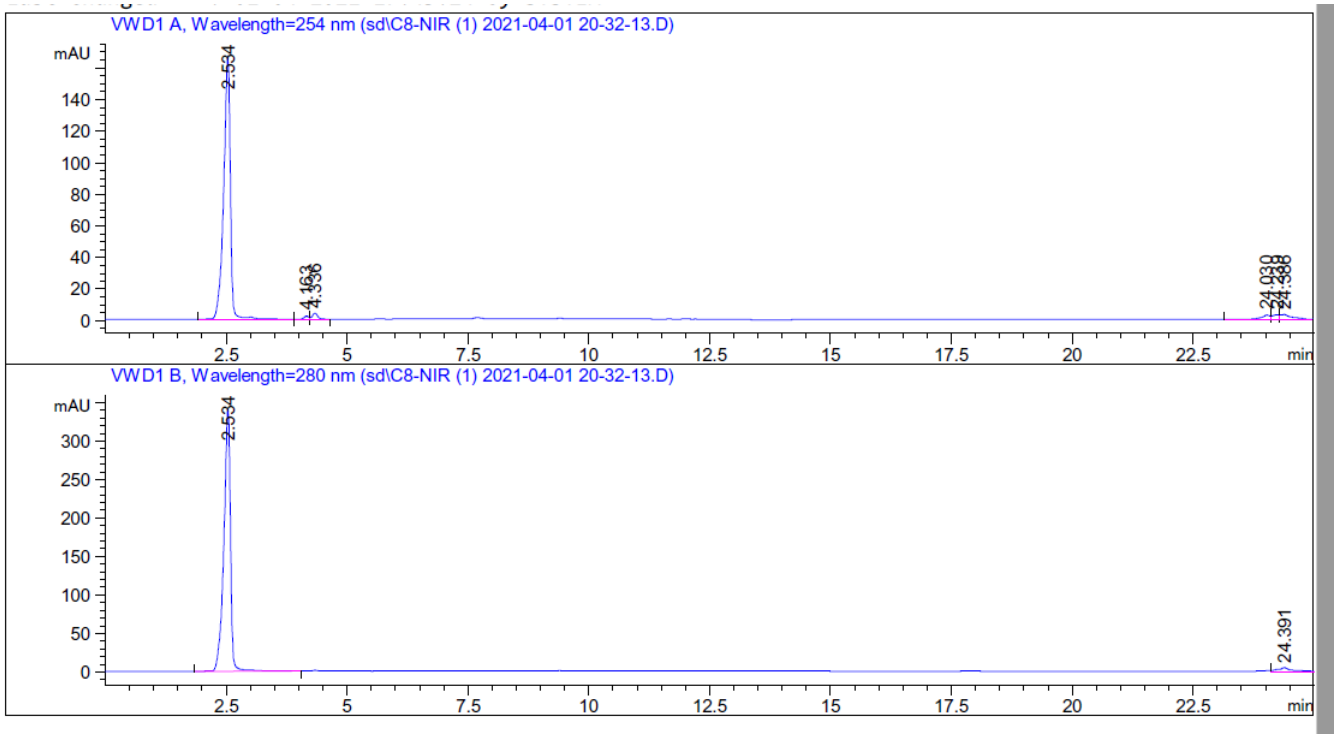

Fig. S23. HPLC trace of compound **nIR8**.

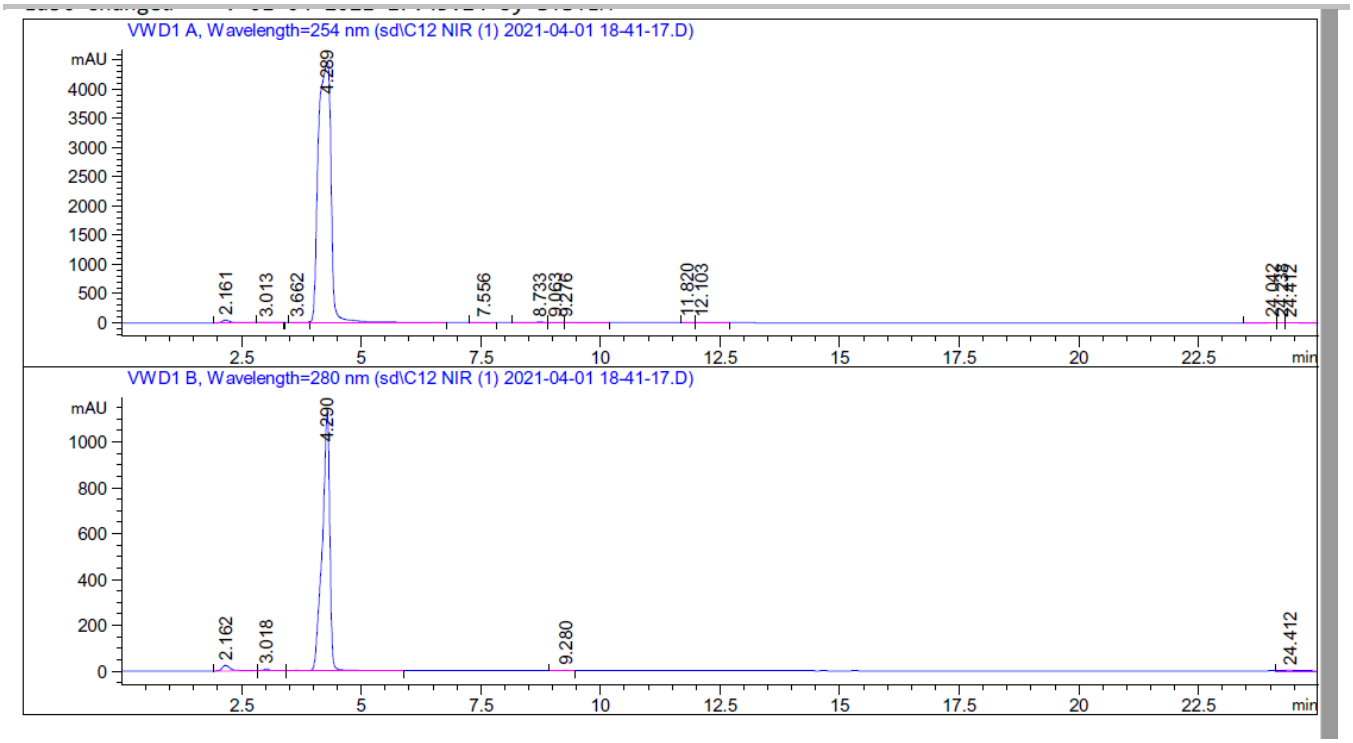

Fig. S24. HPLC trace of compound **nIR12**.

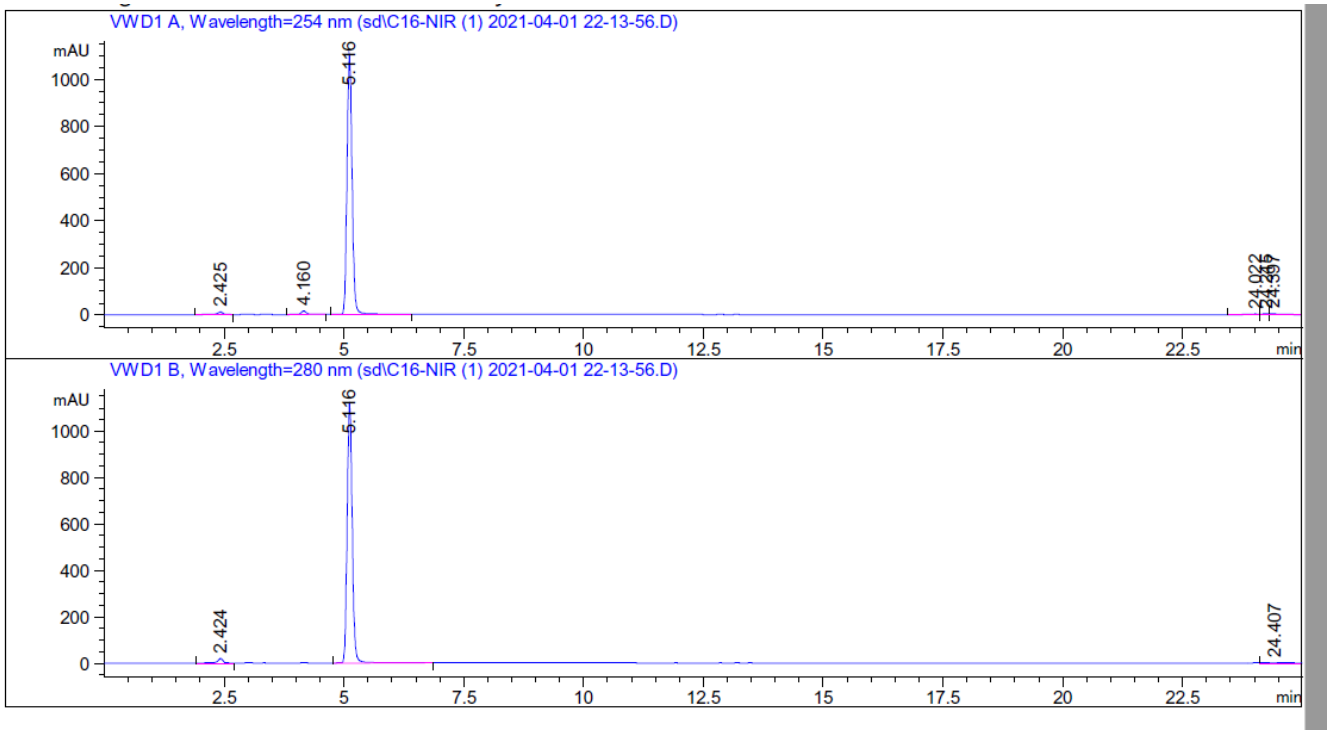

Fig. S25. HPLC trace of compound **nIR16**.

References

1. T. Pastierik, P. Sebej, J. Medalova, P. Stacko and P. Klan, *J. Org. Chem.*, 2014, **79**, 3374-3382.
2. S. Dey, A. Patel, K. Raina, N. Pradhan, O. Biswas, R. Thummer and D. Manna, *Chem. Commun.*, 2020, **56**, 1661-1664.
3. A. Saha, S. Panda, N. Pradhan, K. Kalita, V. Trivedi and D. Manna, *Chem. Eur. J.*, 2018, **24**, 1121-1127.
4. R. Kumar, V. G. Iyer and W. Im, *Abstr. Pap. Am. Chem. S*, 2007, **233**, 273-273.
5. J. M. Wang, R. M. Wolf, J. W. Caldwell, P. A. Kollman and D. A. Case, *J. Comput. Chem.*, 2004, **25**, 1157-1174.
6. J. B. Klauda, R. M. Venable, J. A. Freites, J. W. O'Connor, D. J. Tobias, C. Mondragon-Ramirez, I. Vorobyov, A. D. MacKerell and R. W. Pastor, *J. Phys. Chem. B*, 2010, **114**, 7830-7843.
7. J. C. Phillips, R. Braun, W. Wang, J. Gumbart, E. Tajkhorshid, E. Villa, C. Chipot, R. D. Skeel, L. Kale and K. Schulten, *J. Comput. Chem.*, 2005, **26**, 1781-1802.
8. W. L. Jorgensen, J. Chandrasekhar, J. D. Madura, R. W. Impey and M. L. Klein, *J. Chem. Phys.*, 1983, **79**, 926-935.
9. T. Darden, D. York and L. Pedersen, *J. Chem. Phys.*, 1993, **98**, 10089-10092.
10. S. Miyamoto and P. A. Kollman, *J. Comput. Chem.*, 1992, **13**, 952-962.
11. P. Majumder, U. Baxa, S. T. R. Walsh and J. P. Schneider, *Angew. Chem. Int. Ed.*, 2018, **57**, 15040-15044.